Phase statistics in non-Gaussian scattering

2006 J. Phys. A: Math. Gen. 39 7621

(http://iopscience.iop.org/0305-4470/39/24/002)

INSTITUTE OF PHYSICS PUBLISHING JOURNAL OF PHYSICS A: MATHEMATICAL AND GENERAL

J. Phys. A: Math. Gen. **39** (2006) 7621–7640 doi:10.1088/0305-4470/39/24/002

Phase statistics in non-Gaussian scattering

Stephen M Watson[1], Eric Jakeman[2] and Kevin D Ridley[3]

[1] Florida Space Institute, Building M6306, Kennedy Space Center, FL 32899, USA
[2] School of Mathematical Sciences, University of Nottingham, University Park, Nottingham NG7 2RD, UK
[3] QinetiQ, Malvern, Worcestershire WR14 3PS, UK

E-mail: swatson@mail.ucf.edu, eric.jakeman@nottingham.ac.uk and kdridley@qinetiq.com

Received 8 February 2006
Published 31 May 2006
Online at stacks.iop.org/JPhysA/39/7621

Abstract

Amplitude weighting can improve the accuracy of frequency measurements in signals corrupted by multiplicative speckle noise. When the speckle field constitutes a circular complex Gaussian process, the optimal function of amplitude weighting is provided by the field intensity, corresponding to the intensity-weighted phase derivative statistic. In this paper, we investigate the phase derivative and intensity-weighted phase derivative returned from a two-dimensional random walk, which constitutes a generic scattering model capable of producing both Gaussian and non-Gaussian fluctuations. Analytical results are developed for the correlation properties of the intensity-weighted phase derivative, as well as limiting probability densities of the scattered field. Numerical simulation is used to generate further probability densities and determine optimal weighting criteria from non-Gaussian fields. The results are relevant to frequency retrieval in radiation scattered from random media.

PACS numbers: 02.20.Uw, 11.30.Pb, 12.60.Jv

1. Introduction

In many communication and remote sensing systems, the desired information is carried in the modulation of the phase of the signal of interest [1, 2]. Perhaps, the most commonly encountered example is frequency-modulated radio transmission, where the carrier is modulated to transmit a baseband signal, most often speech [3]. Recovery of the transmitted information is possible through frequency demodulation, an inverse problem of longstanding interest, which outputs the time derivative of the signal phase. A similar problem was found to arise in the determination of particle mobilities using laser light scattering [4]. In this method, coherent light carries a fringe-crossing frequency caused by the drift of particles through a suspension that is subject to an electric field. In addition to the linear motion induced by the applied field, the particles are subject to random Brownian motion that leads

to multiplicative noise in the detected signal. A new element is thereby introduced in the frequency demodulation problem, multiplicative speckle noise [5]. The detected light in this system can be represented mathematically as

$$S(t) = A(t)\exp[\mathrm{i}(\phi(t) + ft)] = E(t)\exp[\mathrm{i}ft], \tag{1}$$

which expresses the frequency of interest f corrupted by the speckle field $E(t)$, where $A(t)$ is the speckle amplitude and $\phi(t)$ is the speckle phase. Frequency demodulation converts this multiplicative noise at the detector into additive noise at the output of the frequency demodulator, i.e.

$$\dot{\vartheta} = f + \dot{\phi}, \tag{2}$$

which is the sum of the quantity of interest f plus a random noise component $\dot{\phi}$. Unfortunately, the phase derivative $\dot{\phi}$ of fully developed speckle is a wildly fluctuating variable [6], and so estimates of f obtained by averaging over (2) are subject to large errors. Recognizing that large spike-like fluctuations in the phase derivative occur when the field amplitude approximates zero, it was proposed that weighting the demodulated signal $\dot{\vartheta}$ by the field amplitude A might improve frequency estimates [4].

Signals of the form (1) are encountered in various communication and remote sensing systems. In principle, one could weight the demodulated signal with an arbitrary function of amplitude $f(A)$ to suppress phase derivative spikes. It was shown in [7] that the variance of the unbiased estimator

$$\hat{f} = \frac{\sum_{n=1}^{N} f(A_n)\dot{\vartheta}_n}{\sum_{n=1}^{N} f(A_n)} = f + \frac{\sum_{n=1}^{N} f(A_n)\dot{\phi}_n}{\sum_{n=1}^{N} f(A_n)}, \tag{3}$$

where n denote statistically independent measurements, is minimized by choice of $f(A) = A^2$ when the speckle field $E(t)$ constitutes a complex Gaussian process. The properties of the intensity-weighted phase derivative statistic, i.e. $J = I\dot{\phi}$, are therefore of interest in this important case. While the analysis was performed assuming a constant frequency offset f, such as that encountered in the mobility measurement experiment, the intensity-weighted result is equally applicable to time-varying frequencies if one performs simultaneous and independent measurements of f with uncorrelated phase noise.

Although the Gaussian process is the most commonly adopted statistical noise model in physics and engineering [8], arising as a manifestation of the central limit theorem, many scattering systems are known to produce non-Gaussian field fluctuations [9]. To investigate how the intensity-weighted phase derivative statistic performs in non-Gaussian regimes, results were also developed from a generic non-Gaussian noise model, namely the deep random phase screen [7]. The phase screen has provided many insights into the scattering problem and has been applied successfully to model radio wave propagation through the ionosphere [10], optical scintillation in the turbulent atmosphere and acoustical propagation in the oceans, amongst others [11].

Another model that has received considerable attention in the context of scattered radiation, and which is capable of producing both Gaussian and non-Gaussian fluctuations, is the random walk [12]. In this approach, the field returned from a random medium is represented as a coherent sum in the complex plane, corresponding to a two-dimensional random walk. The ensuing mathematical problem is equivalent to that posed by Pearson a century ago [13], which continues to be of considerable impact and utility in the sciences and engineering. While the model does not represent a rigorous solution to Maxwell's equations, it has a sound physical basis and has contributed significantly towards our understanding of the scattering problem. Numerous investigations have considered the resultant step length

or amplitude of such random walks, whose square or intensity is of principal interest in direct detection systems [14]. However, it would appear that the corresponding phase-related properties have attracted relatively little attention. In this paper, we develop phase-related results, appropriate to frequency retrieval in scattered coherent radiation, from the random walk model.

In section 2, we introduce the random walk model and discuss its applicability to various scattering systems. In section 3, we obtain the correlation properties and variance of the J statistic, which returns the optimal frequency estimate when the field constitutes a complex Gaussian process, in both Gaussian and non-Gaussian regimes. Given that measures of system performance often require knowledge of detected field probability densities, in section 4 we develop certain limiting densities of the scattered field. Analytical progress beyond these limiting results is difficult, so in section 5 we investigate the problem using numerical simulation. The simulation technique allows for a full investigation of the scattered field, including optimal weighting criteria in non-Gaussian scenarios. In section 6, we close with a brief summary and conclusions.

2. The random walk scattering model

When modelling the scattering of coherent radiation, it is most appropriate to study the properties of the two-dimensional random walk [12]

$$E(\tilde{r},t)=\sqrt{I(\tilde{r},t)}\exp[\mathrm{i}\phi(\tilde{r},t)]\exp(\mathrm{i}\omega t)=\sum_{n=1}^{N}a_n(\tilde{r},t)\exp[\mathrm{i}\theta_n(\tilde{r},t)]\exp(\mathrm{i}\omega t), \tag{4}$$

where $I(\tilde{r},t)$ and $\phi(\tilde{r},t)$ are the intensity and random phase of a complex field $E(\tilde{r},t)$ detected at position $\tilde{r}$ and time t. a_ns are real scattering amplitudes, which depend upon the properties of the scattering centres, θ_ns are phase shifts corresponding to the path length between the detector and those scattering centres, and ω is the radiation frequency. It is important to recognize that the phase of the detected field ϕ is, in general, quite different from the scatterer phase shifts θ_n. Given that we are most interested in the dynamic properties of the resulting field, we shall simplify the following results by suppressing the explicit position dependence $\tilde{r}$, which nevertheless manifests in the phase shifts θ_n. The representation (4) provides an appealing model for particle scattering [14], though has also been applied to continuum scatterers, such as rough surfaces [12], diffusers and extended random media [15]. While the physical applicability of this discrete model is less obvious in the case of continuum scatterers, there is compelling evidence that it nevertheless provides a useful representation in certain circumstances. In such cases, the independent field contributions can be associated with the characteristic scattering scale or correlation length of the continuous random medium. In this paper, we shall consider a_ns and θ_ns to be statistically identical and independent random variables, which will be valid in cases of identical non-interacting particles and continuous random media when the illuminated volume or surface exceeds its characteristic scale length.

In electromagnetic scattering from particulate media and rough surface scattering when the wavelength of the radiation is smaller than the dimension of the surface inhomogeneities, it is often assumed that the independent field contributions in the random walk have no preferred orientation. This corresponds to phase shifts θ that are uniformly distributed when wrapped on the interval $[-\pi,\pi)$, which results in an unbiased two-dimensional random walk. In rough surface scattering, the surface height profiles and resulting phase shifts are often considered to

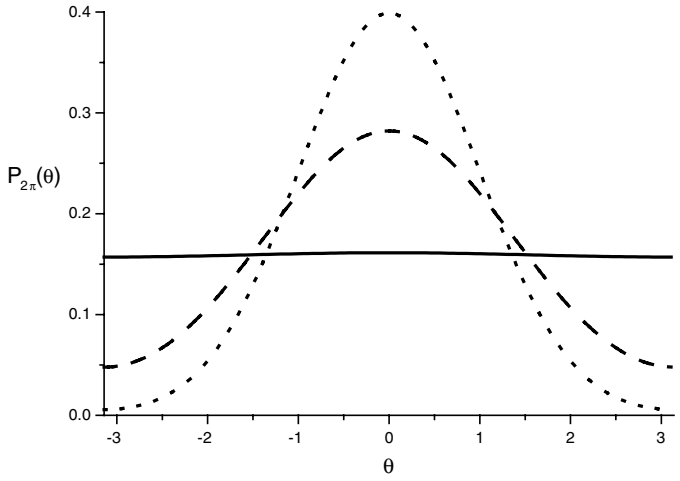

Figure 1. Wrapped phase shift density, i.e. equation (8), with various phase shift variances: dotted curve $\langle\theta^2\rangle = 1$, dashed curve $\langle\theta^2\rangle = 3$ and solid curve $\langle\theta^2\rangle = 10$.

constitute Gaussian processes, such that the single interval phase shifts are Gaussian distributed [12], i.e.

$$p(\theta) = \frac{\exp(-\theta^2/2\langle\theta^2\rangle)}{\sqrt{2\pi\langle\theta^2\rangle}}, \tag{5}$$

where $\langle\theta^2\rangle$ is the phase shift variance. The Gaussian phase shift assumption is also encountered in wave propagation through random media, where phase shifts arise as the path integral over refractive index variations [15]. When representing the scattered field as a two-dimensional random walk, the terms in (4) are combined with their phase shifts modulo-2π, such that they reside in the same branch of the complex plane. It is therefore most appropriate to consider the wrapped density

$$p_{2\pi}(\theta) = \sum_{n=-\infty}^{\infty} p(\theta + 2n\pi) = \frac{\exp(-\theta^2/2\langle\theta^2\rangle)}{\sqrt{2\pi\langle\theta^2\rangle}} \sum_{n=-\infty}^{\infty} \exp\left[-\frac{(2n\pi\theta + 2n^2\pi^2)}{\langle\theta^2\rangle}\right], \tag{6}$$

which exists on the interval $\theta \in [-\pi, \pi)$. While this is readily expressed as an infinite sum over hyperbolic cosine terms, a more useful representation follows from the Poisson sum formula [16], i.e.

$$p_{2\pi}(\theta) = \frac{\exp(-\theta^2/2\langle\theta^2\rangle)}{\sqrt{2\pi\langle\theta^2\rangle}} \sum_{n=-\infty}^{\infty} \int_{-\infty}^{\infty} \exp\left[-\frac{(2x\pi\theta + 2x^2\pi^2)}{\langle\theta^2\rangle}\right] \exp(-\mathrm{i}2\pi nx)\,\mathrm{d}x, \tag{7}$$

resulting in the phase shift density modulo-2π:

$$p_{2\pi}(\theta) = \frac{1}{2\pi}\left\{1 + 2\sum_{n=1}^{\infty} \exp\left(-\frac{n^2\langle\theta^2\rangle}{2}\right)\cos(n\theta)\right\}. \tag{8}$$

The result is greater than the uniform density between $-\pi/2$ and $\pi/2$, and less than it on the remainder of the interval. However, when the phase shift variance $\langle\theta^2\rangle > 10$, the difference between the two is negligible, and the phase shift modulo-2π can be assumed uniform over the entire interval, as shown in figure 1.

While the Gaussian density (5) is appealing in the context of certain scattering systems, one might expect any arbitrary phase shift density $p(\theta)$ to approximate a uniform density when folded under similar conditions, i.e. $p_{2\pi}(\theta) = 1/2\pi$. An unbiased dynamic random walk is therefore likely to emerge whenever the motions of independent scattering centres exceed the radiation wavelength. This will be the case in many high-frequency scattering systems, such as electromagnetic propagation through turbid and turbulent media [15] and laser light scattering from vibrating surfaces [17].

3. Correlation properties of the intensity-weighted phase derivative

Given that the intensity-weighted phase derivative statistic returns the optimal frequency estimate whenever the speckle field $E(t)$ constitutes a complex Gaussian process [7], it is of interest to obtain its correlation properties and variance for the model under study (4). For the complex field $E = X + \mathrm{i}Y$, where X and Y are the in-phase and quadrature components of the field, respectively, the intensity-weighted phase derivative follows as

$$J = I\dot{\phi} = (X^2 + Y^2)\frac{\mathrm{d}}{\mathrm{d}t}\arctan\left[\frac{Y}{X}\right] = X\dot{Y} - Y\dot{X}, \tag{9}$$

which requires the field to be a differentiable process. While there are mathematical models for which the first and higher order derivatives do not exist, physical systems invariably deviate from such abstract idealizations. In practice, it is almost always possible to construct a quantity that approximates a derivative, which requires a sampling rate sufficiently high to resolve the characteristic scale or correlation time of the system under study. For the idealized case of scattering from particles undergoing Brownian motion, the returned phase is continuous yet non-differentiable, and so it is preferable to characterize phase changes in terms of phase differences $\delta\phi$. Taking advantage of the statistical independence between the amplitude A and the amplitude-weighted phase difference $A\delta\phi$ when the scattered field constitutes a complex Gaussian process [4], one can adopt a similar procedure to that outlined in [7] and show that the intensity-weighted phase difference $I\delta\phi$ is now optimal when extracting a frequency offset f. For sufficiently high sampling rates, the discrepancy between the phase difference $\delta\phi$ and the phase derivative $\dot{\phi}$ becomes one of mathematical formality; hence, we shall proceed with the phase derivative in analytical developments, though encounter the phase difference in numerical simulations due to their discrete nature.

The intensity-weighted phase derivative statistic can also be expressed as

$$J = \mathrm{Im}\left(E^*\frac{\partial E}{\partial t}\right) = \frac{1}{2\mathrm{i}}\left(E^*\frac{\partial E}{\partial t} - E\frac{\partial E^*}{\partial t}\right), \tag{10}$$

which is reminiscent of the flux density obtained from the continuity equation [16] and is identical to a quantity recently investigated in the context of phase reconstruction [18]. The intensity-weighted phase derivative for the random walk follows by inserting (4) into (10), i.e.

$$\begin{aligned} J(t) &= \frac{1}{2}\sum_{n,m=1}^{N}\dot{\theta}_m a_n(t)a_m(t)\{\exp(\mathrm{i}[\theta_n(t) - \theta_m(t)]) + \exp(-\mathrm{i}[\theta_n(t) - \theta_m(t)])\} \\ &= \sum_{n,m=1}^{N}\dot{\theta}_m a_n(t)a_m(t)\cos[\theta_n(t) - \theta_m(t)], \end{aligned} \tag{11}$$

where $\dot{\theta}_m$ correspond to the phase shift derivatives of individual scattering centres, which will be proportional to their velocities. Continuing with the exponential representation, the J

statistic correlation function requires evaluating the ensemble average

$$\langle J(t)J(t')\rangle = \frac{1}{4}\Bigg\langle \sum_{n,m,p,q=1}^{N} \dot\theta_m(t)\dot\theta_q(t)a_n(t)a_m(t)a_p(t')a_q(t') \times (\exp(\mathrm{i}[\theta_n(t)-\theta_m(t)]) + \exp(-\mathrm{i}[\theta_n(t)-\theta_m(t)])) \times (\exp(\mathrm{i}[\theta_p(t')-\theta_q(t')]) + \exp(-\mathrm{i}[\theta_p(t')-\theta_q(t')]))\Bigg\rangle. \tag{12}$$

Progress can be made by assuming that a_ns, θ_ns and $\dot\theta_m$s are statistically identical and independent random variables, corresponding to statistically identical scatterers whose individual scattering amplitudes, positions and velocities are independent. We shall further assume that $\dot\theta_m$s are zero mean, corresponding to an equal likelihood of particle motion in all directions, which simplifies the above expression to

$$\begin{aligned}\langle J(t)J(t')\rangle = \frac{\langle\dot\theta(t)\dot\theta(t')\rangle}{4} \sum_{n,m,p=1}^{N} \langle a_n(t)a_m(t)a_p(t')a_m(t')\rangle \\ \times \langle \exp(\mathrm{i}[\theta_n(t)-\theta_m(t)+\theta_p(t')-\theta_m(t')]) \\ + \exp(-\mathrm{i}[\theta_n(t)-\theta_m(t)+\theta_p(t')-\theta_m(t')]) \\ + \exp(\mathrm{i}[\theta_n(t)-\theta_m(t)-\theta_p(t')+\theta_m(t')]) \\ + \exp(-\mathrm{i}[\theta_n(t)-\theta_m(t)-\theta_p(t')+\theta_m(t')])\rangle,\end{aligned} \tag{13}$$

where we have grouped the exponential phase terms into conjugate pairs, and recognize the phase shift derivative correlation function of the scatterers $\langle\dot\theta(t)\dot\theta(t')\rangle$. Averaging over the phase terms θ_n, which for an unbiased dynamic random walk are uniformly distributed on the interval $[-\pi,\pi)$, returns contributions of $N\langle a^2(t)a^2(t')\rangle$ from each of the four factors in (13) when $n = p = m$ and contributions of $N(N-1)\langle a(t)a(t')\rangle^2$ $\langle\exp(\mathrm{i}[\theta(t)-\theta(t')])\rangle\langle\exp(-\mathrm{i}[\theta(t)-\theta(t')])\rangle$ from the lower conjugate pair when $n = p \neq m$. All other terms in the summation yield zero contribution. Identifying the field correlation function

$$g^{(1)}(t,t') = \frac{\langle E(t)E(t')\rangle}{[\langle I(t)\rangle\langle I(t')\rangle]^{1/2}} = \frac{\langle a(t)a(t')\rangle\langle\exp(\mathrm{i}[\theta(t)-\theta(t')])\rangle}{[\langle a^2(t)\rangle\langle a^2(t')\rangle]^{1/2}}, \tag{14}$$

where $\langle I(t)\rangle = N\langle a^2(t)\rangle$ is the mean intensity, normalizes the sum of these six non-zero contributions to

$$\frac{\langle J(t)J(t')\rangle}{\langle I(t)\rangle\langle I(t')\rangle} = \langle\dot\theta(t)\dot\theta(t')\rangle\left\{\frac{|g^{(1)}(t,t')|^2}{2} + \frac{1}{N}\left(\frac{\langle a^2(t)a^2(t')\rangle}{\langle a^2(t)\rangle\langle a^2(t')\rangle} - \frac{|g^{(1)}(t,t')|^2}{2}\right)\right\}. \tag{15}$$

It is interesting to compare this result with that for the intensity correlation function [9]

$$g^{(2)}(t,t') = \frac{\langle I(t)I(t')\rangle}{\langle I(t)\rangle\langle I(t')\rangle} = (1+|g^{(1)}(t,t')|^2) + \frac{1}{N}\left(\frac{\langle a^2(t)a^2(t')\rangle}{\langle a^2(t)\rangle\langle a^2(t')\rangle} - 1 - |g^{(1)}(t,t')|^2\right). \tag{16}$$

We note that results (15) and (16) apply to an arbitrary number of scatterers whose wrapped phase shift densities are uniform, i.e. $p_{2\pi}(\theta) = 1/2\pi$.

For a large number of scatterers N, corresponding to a circular complex Gaussian field, the normalized intensity-weighted phase derivative correlation function (15) simplifies to

$$\frac{\langle J(t)J(t')\rangle}{\langle I(t)\rangle\langle I(t')\rangle} = \langle\dot\theta(t)\dot\theta(t')\rangle\frac{|g^{(1)}(t,t')|^2}{2}. \tag{17}$$

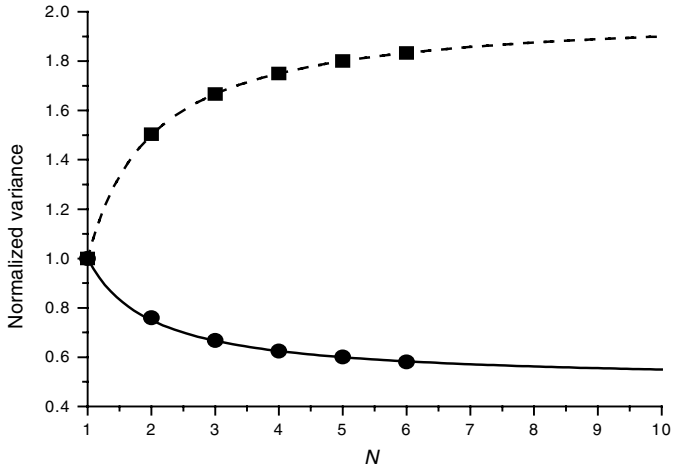

Figure 2. Normalized variances of intensity $\langle I^2\rangle/\langle I\rangle^2$ (dashed line) and intensity-weighted phase derivative $\langle J^2\rangle/(\langle I\rangle^2\langle\dot\theta^2\rangle)$ (solid line) with increasing scatterer number N. The squares and circles are corresponding simulation results.

The corresponding intensity correlation function (16) reduces to the well-known Siegert factorization theorem [19]

$$g^{(2)}(t,t') = 1 + |g^{(1)}(t,t')|^2, \tag{18}$$

which allows the modulus of the field correlation $g^{(1)}(t,t')$ to be determined from the more readily detected intensity correlation function $g^{(2)}(t,t')$. Inserting (18) into (17) obtains the following expression for the correlation of J in the Gaussian limit:

$$\langle J(t)J(t')\rangle = \frac{\langle\dot\theta(t)\dot\theta(t')\rangle}{2}(\langle I(t)I(t')\rangle - \langle I(t)\rangle\langle I(t')\rangle). \tag{19}$$

Results (15) and (16) also return the normalized variances of the intensity-weighted phase derivative J and intensity I for arbitrary scattering number N, i.e. in non-Gaussian regimes. Assuming that the scattering amplitudes are of fixed and equal size, a normalized variance of the intensity-weighted phase derivative can be defined as

$$\frac{\langle J^2\rangle}{\langle I\rangle^2\langle\dot\theta^2\rangle} = \frac{1}{2}\left(1 + \frac{1}{N}\right), \tag{20}$$

where $\langle\dot\theta^2\rangle$ is the variance of the scatterers' phase shift derivative and the corresponding result for the intensity variance is

$$\frac{\langle I^2\rangle}{\langle I\rangle^2} = 2 - \frac{1}{N}. \tag{21}$$

The normalized variances of the intensity and J statistic are plotted in figure 2 against increasing scatterer number N. The intensity returned from a single scatterer does not fluctuate, so has a normalized variance of unity. When a large number of scatterers are present, which results in a circular complex Gaussian process, the intensity fluctuations are exponentially distributed with normalized variance 2. By contrast, the normalized variance of the J statistic falls to half the value of one scatterer in the Gaussian limit. When only one scatterer is present, the detected field intensity is constant, and so the variance of J is due solely to the individual scatterers' phase shift derivative, i.e. $\langle\dot\theta^2\rangle$. It is interesting that for a

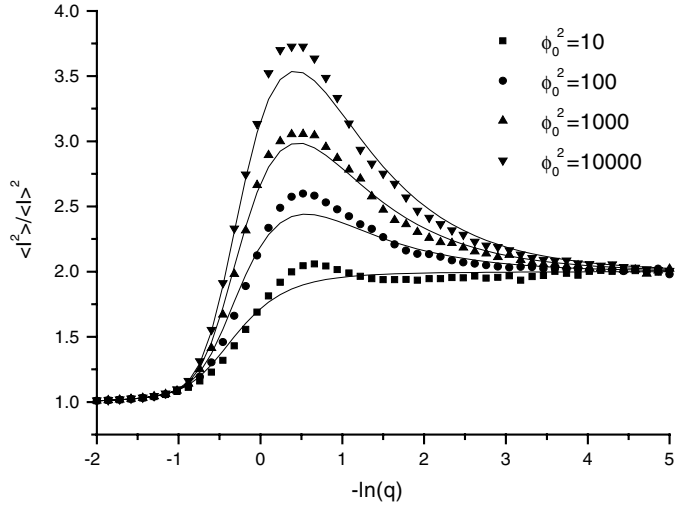

Figure 3. Normalized variance of intensity beyond a Gaussian-correlated deep random phase screen. Results are plotted against the dimensionless propagation distance $q = k\xi^2/2z\phi_0\sqrt{6}$, where z is the distance, k is the radiation wave number, ξ is the screen's correlation length and ϕ_0 is its rms phase modulation depth. Lines are analytical approximations (see [7]).

large number of scatterers, when the field's amplitude and phase fluctuate due to interference between the returned field contributions, the variance of the estimator $\langle J^2 \rangle$ falls to half this value. In this Gaussian limit, the fields' phase derivative $\langle \dot{\phi}^2 \rangle$ is known to have infinite variance [6], which causes large errors when determining f by averaging over (2). An equivalent result was found following scattering from a deep random phase screen [7], for which the intensity and J statistic variances are plotted against increasing dimensionless propagation distance in figures 3 and 4. In comparison to the random walk results, the curves following scattering from a smoothly varying random phase screen exhibit regions of heightened non-Gaussian fluctuations. These occur in the so-called focusing regime, which arises due to the focusing effects of the screen's smooth lens-like inhomogeneities. It was previously shown that the optimal weighting in this focusing regime can deviate significantly from that of the Gaussian limit statistic. Given that the random walk was constructed from independent and unbiased field contributions, the resulting field will not exhibit such heightened fluctuations and is therefore similar to scattering from a diffuse, non-focusing phase screen [9, 11].

4. Probability densities of scattered field parameters

While the above correlation properties provide insight into the scattering process, probability densities of scattered field parameters are useful when determining system performance measures such as false alarm rates and misdetection probabilities. The field scattered from a large number of particles, i.e. $N \to \infty$, is known to constitute a circular complex Gaussian process. The probability density function (PDF) of the phase derivative in this Gaussian limit then follows from the result of Rice for a differentiable complex Gaussian process [6]

$$p_{\mathrm{G}}(\dot{\phi}) = \frac{\tau_{\mathrm{c}}/2}{\left(1 + \tau_{\mathrm{c}}^2 \dot{\phi}^2\right)^{3/2}}, \tag{22}$$

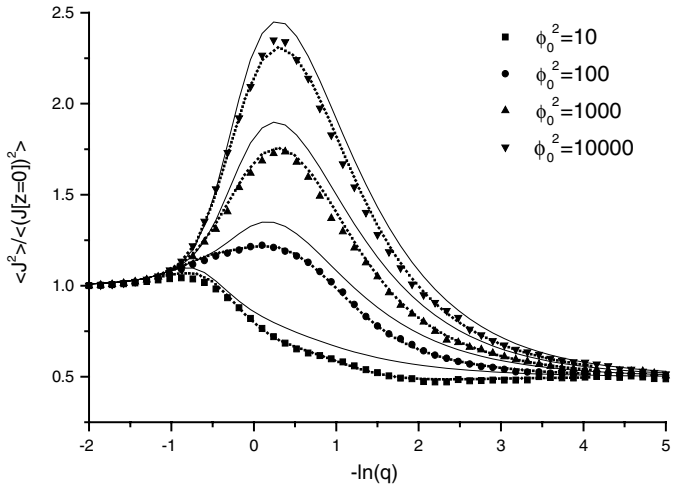

Figure 4. Same as figure 3 but for J statistic. Dotted lines are the results of numerical integration (see [7]).

where τ_c given by $\tau_c^{-2} = -(d^2/dt^2)g^{(1)}(t)|_{t=0}$ can be interpreted as a field correlation time [7]. The PDF has undefined variance, symptomatic of the extreme fluctuations in this quantity, and a spread $\langle|\dot{\phi}|\rangle = 1/\tau_c$. The corresponding J statistic PDF can be obtained under the same assumptions, resulting in the symmetric negative exponential density [7]

$$p_G(J) = \frac{1}{2\langle|J|\rangle} \exp\left(-\frac{|J|}{\langle|J|\rangle}\right), \tag{23}$$

where $\langle|J|\rangle = (\langle I\rangle/2\tau_c)$. The intensity PDF is governed by the well-known result

$$p_G(I) = \frac{\exp(-I/\langle I\rangle)}{\langle I\rangle}, \tag{24}$$

where $\langle I\rangle$ is the mean intensity. Probability densities for the intensity I, phase derivative $\dot{\phi}$ and J statistic of a complex Gaussian field are plotted in figures 5(*e*), 8 and 9, respectively. It is interesting that the intensity and J statistic densities scale with the number of steps in the random walk N, whereas the phase derivative density (22) is independent of this quantity. This is because the phase derivative of a complex process is dependent on the ratios of in-phase and quadrature components, as opposed to their absolute magnitudes.

Progress with field densities from an arbitrary number of scatterers N requires the scatterer phase shift properties to be specified. The assumption of jointly Gaussian statistics is appealing in the context of certain scattering systems and simplifies mathematical calculations. The single interval phase is then Gaussian distributed (5), which wraps to that form required of an unbiased random walk, i.e. $p_{2\pi}(\theta) = 1/2\pi$, when $\langle\theta^2\rangle > 10$. Clearly, this choice of single interval density is not unique and other forms could be adopted: one alternative being the von Mises density, which has been applied in random walk approaches to electromagnetic scattering [20]. However, the joint Gaussian assumption also simplifies the phase shift's higher order properties, which are required for the phase derivative and J statistic.

The simplest non-Gaussian field results are obtained from a single scatterer, when the intensity is fixed at unity, so has no effect when weighting the demodulator output. The J statistic then assumes the statistical properties of the fields' phase derivative $\dot{\phi}$, which equals the scatterer phase shift derivative $\dot{\theta}$ in this simplest case. For phase shifts that constitute

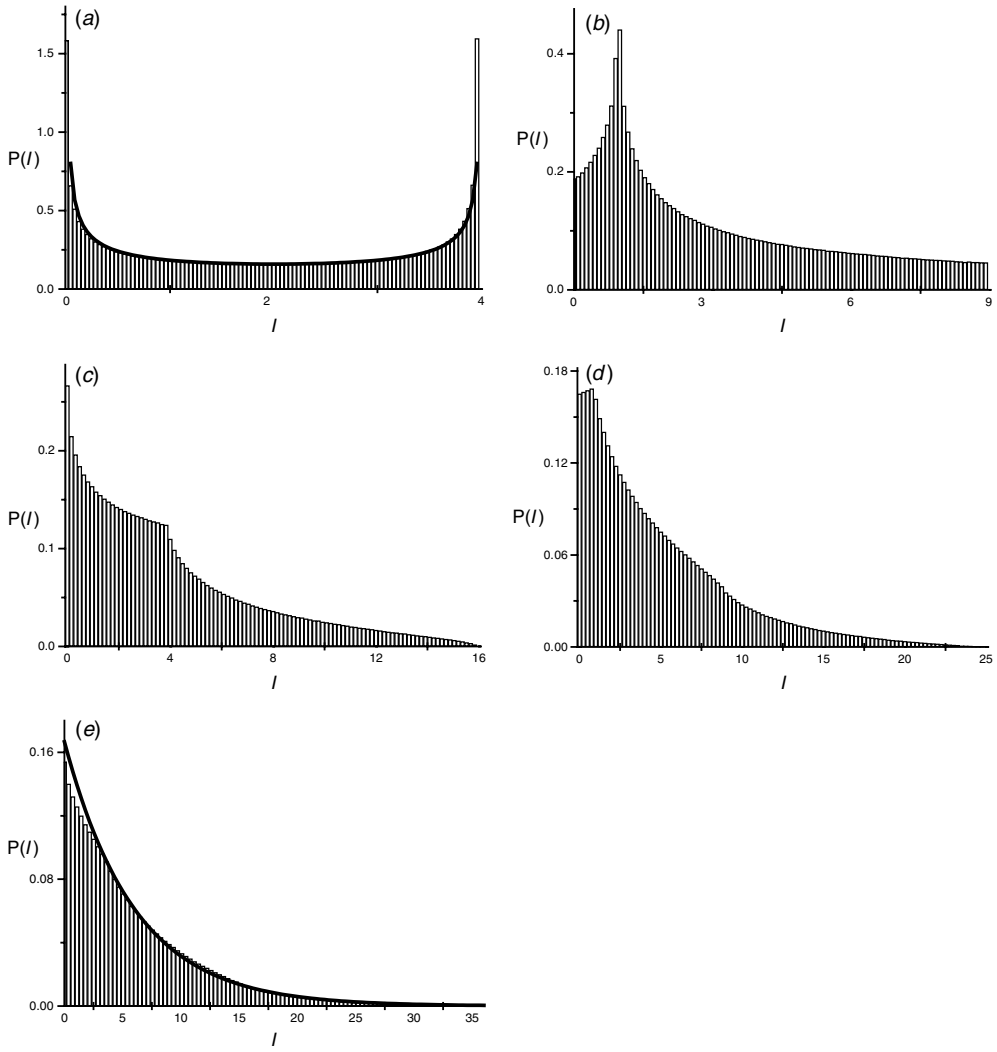

Figure 5. Probability densities for intensity from (*a*) two, (*b*) three, (*c*) four, (*d*) five and (*e*) six scatterers. Parts (*a*) and (*e*) also display theoretical curves from equations (36) and (24), respectively.

Gaussian processes, the phase shift derivative $\dot{\theta}$ will be Gaussian distributed, resulting in the densities

$$p_1(J) = p_1(\dot{\phi}) = p(\dot{\theta}) = \frac{\exp(-\dot{\theta}^2/2\langle\dot{\theta}^2\rangle)}{\sqrt{2\pi\,\langle\dot{\theta}^2\rangle}}. \tag{25}$$

Probability densities of $\dot{\phi}$ and J for one scatterer are plotted in figures 6 and 7, respectively, in which the phase shift derivative variance $\langle\dot{\theta}^2\rangle = 0.02$.

It is interesting that the phase shift derivative variance of an individual scatterer, i.e. $\langle\dot{\theta}^2\rangle$, can be related to the correlation time τ_c of the complex Gaussian field that arises from a large

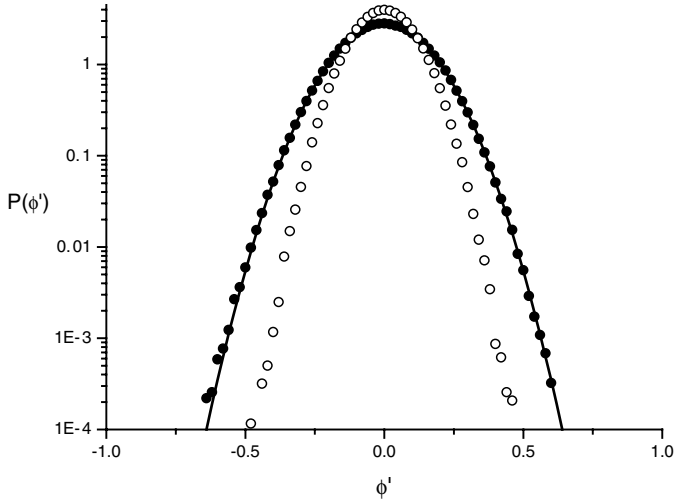

Figure 6. Phase derivative densities for one (solid circles) and two (open circles) scatterers. The curve is the theoretical phase shift derivative density, i.e. equation (25) with $\langle\dot{\theta}^2\rangle = 0.02$.

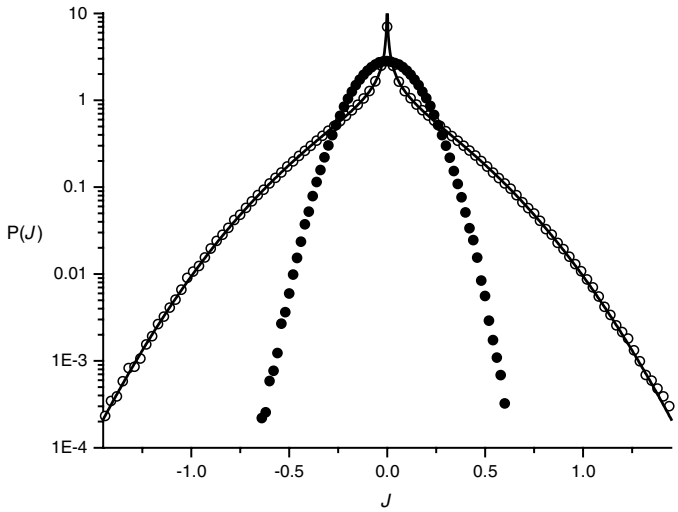

Figure 7. Same as figure 6 but for J statistic. The theoretical curve represents equation (33).

number of scatterers. When the scatterers are of fixed and equal amplitude, and the phase constitutes a Gaussian process, the field correlation (14) simplifies to

$$g^{(1)}(t) = \exp(-\langle\theta^2\rangle[1 - \rho_\theta(t)]), \tag{26}$$

where $\rho_\theta(t) = \langle\theta(t)\theta(0)\rangle/\langle\theta^2\rangle$ is the phase shift correlation function. The field correlation time then follows from

$$\frac{1}{\tau_c^2} = -\frac{\mathrm{d}^2}{\mathrm{d}t^2} g^{(1)}(t)\bigg|_{t=0} = -\langle\theta^2\rangle \frac{\mathrm{d}}{\mathrm{d}t}\left(\langle\theta^2\rangle + \frac{\mathrm{d}}{\mathrm{d}t}\right)\rho_\theta(t)\bigg|_{t=0} = \langle\dot{\theta}^2\rangle, \tag{27}$$

where we have recognized that a stationary random process and its derivative are uncorrelated, i.e. $\langle\dot{\theta}(t)\theta(t)\rangle = 0$. This result also relates the phase derivative density's spread (22) to the rms phase shift derivative of a single scatterer, i.e. $\langle|\dot{\phi}|\rangle = \sqrt{\langle\dot{\theta}^2\rangle}$.

For two scatterers of fixed and equal amplitude, say unity, results can be developed from their in-phase and quadrature components, i.e.

$$X = \cos\theta_1 + \cos\theta_2 \qquad \text{and} \qquad Y = \sin\theta_1 + \sin\theta_2. \tag{28}$$

The fields' phase derivative then follows from (9) and (28) as

$$\dot{\phi} = \frac{X\dot{Y} - Y\dot{X}}{X^2 + Y^2} = \frac{(\dot{\theta}_1 + \dot{\theta}_2)}{2}, \tag{29}$$

which reveals that the phase derivative density returned from two equal scatterers is also Gaussian, though rather surprisingly, with half the variance of one scatterer, i.e. $\langle\dot{\phi}^2\rangle = \langle\dot{\theta}^2\rangle/2$. The J statistic for two scatterers is

$$J = X\dot{Y} - Y\dot{X} = (\dot{\theta}_1 + \dot{\theta}_2)(1 + \cos[\theta_1 - \theta_2]). \tag{30}$$

The probability density of J can be developed from its characteristic function, which averaging over the uniform phase difference density for $[\theta_1 - \theta_2]$ results in

$$\begin{aligned} C_2(\lambda) &= \left\langle \frac{\exp(\mathrm{i}\lambda[\dot{\theta}_1 + \dot{\theta}_2])}{2\pi} \int_0^{2\pi} \exp(\mathrm{i}\lambda[\dot{\theta}_1 + \dot{\theta}_2]\cos[\theta_1 - \theta_2])d[\theta_1 - \theta_2] \right\rangle \\ &= \langle \exp(\mathrm{i}\lambda[\dot{\theta}_1 + \dot{\theta}_2]) J_0(\lambda[\dot{\theta}_1 + \dot{\theta}_2])\rangle, \end{aligned} \tag{31}$$

where $J_n(z)$ is a Bessel function [21]. The characteristic function (31) can be simplified by recognizing that the sum of two Gaussian random variables is another Gaussian variable with twice the variance, i.e. $\dot{\theta}_1 + \dot{\theta}_2 = s$, where $\langle s^2\rangle = 2\langle\dot{\theta}^2\rangle$. The required density then follows by averaging over the Gaussian phase derivative variable s and inverse Fourier transforming, i.e.

$$p_2(J) = \frac{1}{2\pi} \int_{-\infty}^{\infty} \exp(\mathrm{i}\lambda J)\,\mathrm{d}\lambda \int_{-\infty}^{\infty} \{\exp(\mathrm{i}\lambda s) J_0(\lambda s)\} \frac{\exp(-s^2/2\langle s^2\rangle)}{\sqrt{2\pi\langle s^2\rangle}}\,\mathrm{d}s. \tag{32}$$

The integrals are fairly straightforward and result in the probability density of the J statistic for two equal scatterers

$$p_2(J) = \frac{1}{\pi^{\frac{3}{2}}} \frac{\exp\left(-J^2/32\langle\dot{\theta}^2\rangle\right)}{\sqrt{32\langle\dot{\theta}^2\rangle}} K_{1/4}\left(\frac{J^2}{32\langle\dot{\theta}^2\rangle}\right), \tag{33}$$

where $K_n(z)$ is a modified Bessel function of the second kind [21]. The density has variance $\langle J^2\rangle = 3\langle\dot{\theta}^2\rangle$ and normalized variance $\langle J^2\rangle/(\langle I\rangle^2\langle\dot{\theta}^2\rangle) = 3/4$, in agreement with equation (20) and figure 2. The density (33) is plotted in figure 7, where it can be seen that the Gaussian term dominates for large values of J. For small J, $K_n(z)$ can be replaced by its small argument approximation [21], resulting in

$$p_2(J) \sim \frac{\Gamma(1/4)}{4\pi^{3/2}\langle\dot{\theta}^2\rangle^{1/4}} |J|^{-1/2}, \qquad J \to 0, \tag{34}$$

where $\Gamma(z)$ is the gamma function [21], which diverges at the origin. The corresponding intensity from two scatterers is

$$I = |\exp(\mathrm{i}\theta_1) + \exp(\mathrm{i}\theta_2)|^2 = 2 + 2\cos(\varphi), \tag{35}$$

where $\varphi = \theta_1 - \theta_2$, whose density is governed by the standard result

$$p_2(I) = p(\varphi)\left|\frac{\mathrm{d}\varphi}{\mathrm{d}I}\right| = \frac{1}{2\pi\sin(\varphi)} = \frac{1}{\pi\sqrt{I(4-I)}}, \tag{36}$$

which is plotted in figure 5(*a*) and is often associated with randomly phased sine waves [1]. It is of interest to note that both the intensity and J statistic densities share the same divergent asymptote at the origin.

Evaluation of the phase derivative density $p_N(\dot{\phi})$ and intensity-weighted phase derivative density $p_N(J)$ is difficult for larger scatterer number N. While the phase derivative can be expressed in terms of in-phase and quadrature components, such as that encountered between (28) and (29), the complex form of this quantity makes analytical progress difficult when $N > 2$. Some progress can be made with the intensity-weighted phase derivative statistic. Returning to (11), the characteristic function of this variable for arbitrary N is

$$\begin{aligned} C_N(\lambda) &= \left\langle \exp\left(\mathrm{i}\lambda \sum_{n,m=1}^{N} \dot{\theta}_m \cos[\theta_n - \theta_m] \right) \right\rangle \\ &= \left\langle \exp\left(\mathrm{i}\lambda \sum_{m=1}^{N} \dot{\theta}_m \right) \prod_{n \neq m=1}^{N} \exp(\mathrm{i}\lambda \dot{\theta}_m \cos[\theta_n - \theta_m]) \right\rangle. \end{aligned} \tag{37}$$

Averaging the phase differences $[\theta_n - \theta_m]$ over a uniform density simplifies this result to

$$C_N(\lambda) = \left\langle \exp\left(\mathrm{i}\lambda \sum_{m=1}^{N} \dot{\theta}_m \right) \prod_{m=1}^{N} J_0^{(N-1)}(\lambda \dot{\theta}_m) \right\rangle = \left\langle \exp[\mathrm{i}\lambda\dot{\theta} + (N-1)\ln[J_0(\lambda\dot{\theta})]] \right\rangle^N, \tag{38}$$

which remains to be averaged over the Gaussian phase shift derivative density (25) and inverse Fourier transformed. While analytical progress is difficult, result (38) may find utility in numerical evaluations. We remark briefly that the corresponding intensity density is given by Kluyver's integral representation [22]

$$p_N(I) = \frac{1}{2} \int_0^\infty u J_0(u\sqrt{I}) J_0^N(u)\, \mathrm{d}u, \tag{39}$$

which follows from the intensity's characteristic function. However, the required averaging and inversion is more straightforward in this case, since unlike the J statistic, the intensity I is independent of the scatterers' phase shift derivative $\dot{\theta}_m$. Kluyver's result can then be evaluated as a Fourier–Bessel series for arbitrary N.

5. Numerical simulation

Analytical progress with the phase derivative $\dot{\phi}$ and intensity-weighted phase derivative J is difficult when more than two scatterers are present. An alternative method of investigation is to numerically simulate the addition of random rotating phasors, corresponding to the sum of scattered field contributions in (4). The simplest scenario, which was adopted to derive the previous probability densities, is to combine phasors of unit amplitude. The dynamic properties of the field then arise solely from constructive and destructive interferences between independent phasors.

The starting point in the simulations is the generation of N independent phase shifts $\{\theta_1, \theta_2, \ldots, \theta_n, \ldots, \theta_N\}$, corresponding to the N scattering centres (4). For an evolving random walk, each individual phase shift θ_n constitutes a sequence of correlated random numbers, i.e. $\theta_n = \{\theta_{n1}, \theta_{n2}, \ldots, \theta_{nM}\}$, which trace the motion of a single scatterer over M time steps Δt. The discrete nature of the simulation technique returns differences, as opposed to mathematical derivatives, though the approximation can be made sufficiently accurate. The set of phase shifts $\{\theta_{1;1,2,\ldots,M}, \ldots, \theta_{n;1,2,\ldots,M}, \ldots, \theta_{N;1,2,\ldots,M}\}$ then represents the evolution of the N scatterers over the observation interval $M\Delta t$. Following from section 4 we shall assume

that the individual phase shifts are Gaussian distributed (5), which allows sequences to be generated using standard numerical techniques. The simplest approach takes delta-correlated Gaussian random numbers and multiplies them by the spectrum of the phase shift correlation function, i.e. $\Im[\langle\theta(t)\theta(0)\rangle]$, where $\Im$ corresponds to a Fourier transform. Application of an inverse Fourier transform then returns a sequence of correlated Gaussian random numbers that constitute a single phase shift realization θ_n. This filtering process requires the phase shift correlation to be specified, a simple candidate being the single scale ξ Gaussian form

$$\langle\theta(t)\theta(0)\rangle = \langle\theta^2\rangle \exp\left(-\frac{t^2}{\xi^2}\right), \tag{40}$$

whose spectrum shares the same functional form. Using the result $\langle\dot{\theta}^2\rangle = -(\mathrm{d}^2/\mathrm{d}t^2)\langle\theta(t)\theta(0)\rangle|_{t=0}$ from equation (27), the corresponding phase shift derivative variance can be identified as $\langle\dot{\theta}^2\rangle = 2\langle\theta^2\rangle/\xi^2$. This parameter fully characterizes the probability densities of $\dot{\phi}$ and J developed in section 4.

Given N independent phase shift sequences, the resultant intensity values can be calculated as

$$I_{N,m} = |E_{N,m}|^2 = |\exp(\mathrm{i}\theta_{1,m}) + \exp(\mathrm{i}\theta_{2,m}) + \cdots + \exp(\mathrm{i}\theta_{N,m})|^2, \tag{41}$$

which will be of length M, and the J statistic as

$$J_{N,m} = \mathrm{Im}\left(E^*_{N,m}\frac{E_{N,m} - E_{N,m-1}}{\Delta t}\right), \tag{42}$$

which will be of length $M - 1$. The phase derivative of the resultant field can be evaluated from the real and imaginary contributions of each of the N independent phasors, though a simpler implementation follows from (41) and (42) as

$$\dot{\phi}_{N,m} = \frac{J_{N,m}}{I_{N,m}} \tag{43}$$

which will be of length $M - 1$.

To preserve the accuracy of the simulation technique, the scattered field contributions should be unambiguously resolved. Visualizing the field from a single scatterer as a unit phasor rotating in the complex plane, it is apparent that the rotation between successive values should be maintained less than π, i.e. $|\theta_{n,m} - \theta_{n,m-1}| \ll \pi$, which for a time step Δt requires $\Delta t|\mathrm{d}\theta/\mathrm{d}t| \ll \pi$. This can be evaluated in an rms sense for the autocorrelation of interest (40) and results in the maximum time step

$$\Delta t_{\max} = \frac{\pi\xi}{\sqrt{2\langle\theta^2\rangle}}. \tag{44}$$

In the simulations, phase shift sequences θ_n of duration $M\Delta t = 2^{13}$ were generated with time step $\Delta t = 1$, correlation length $\xi = 100$ and variance $\langle\theta^2\rangle = 100$. Following from equation (8) and figure 1, the folded phase density of individual sequences $p_{2\pi}(\theta)$ can be assumed uniform on $[-\pi, \pi)$, and so the coherent sum of phasors will perform an unbiased dynamic random walk. The rms phase shift derivative with these parameters, i.e. $\sqrt{\langle\dot{\theta}^2\rangle} = \sqrt{0.02} \approx 0.14$, is significantly smaller than the maximum phase difference π, which is reflected in the maximum time step $\Delta t_{\max} \approx 22$ being significantly greater than that of the simulations $\Delta t = 1$.

The sequences returned from the simulations can be binned to produce full probability densities for the intensity I, phase derivative $\dot{\phi}$ and J statistic. All densities were obtained by binning results from 1000 independent field realizations. The intensity PDF of one scatterer is a delta function positioned at unity. The intensity PDFs of 2–6 scatterers are plotted in figure 5. The results for two, three and four scatterers can be seen to deviate significantly

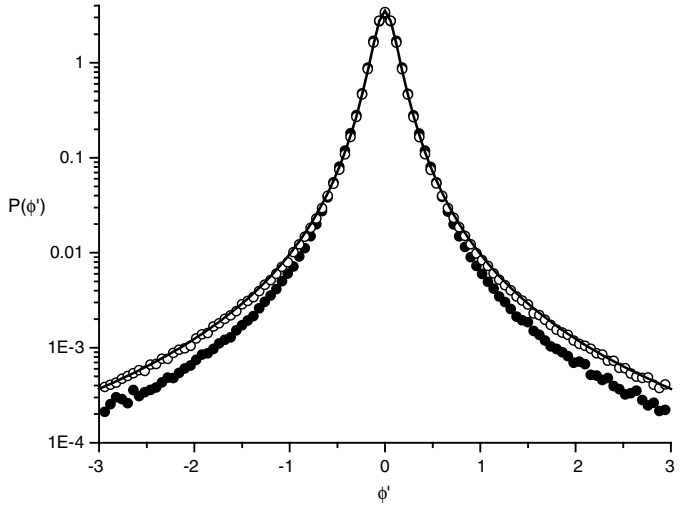

Figure 8. Phase derivative densities for three (solid circles) and six scatterers (open circles). The curve is the theoretical prediction for a complex Gaussian process, i.e. equation (22).

from the negative exponential form predicted in the Gaussian limit, i.e. equation (24). The complex form of these densities is dependent on the number of ways that phasors can construct to yield a given intensity value. While the intensity is always confined to be less than N^2, the returns from five or more scatterers, corresponding to the intensities plotted in figures 5(*d*) and (*e*), are often assumed to approximate a complex Gaussian process [23]. We also note that the intensity PDFs compare favourably with previous evaluations of their corresponding Fourier–Bessel series [24]. The phase derivative PDFs from one and two scatterers are plotted in figure 6. As predicted by equation (29), the phase derivative returned from two scatterers is also Gaussian distributed, though with half the variance of one scatterer. The PDFs for three and six scatterers are plotted in figure 8, both of which are heavy-tailed distributions that indicate $\dot{\phi}$ is a wildly fluctuating variable even for small scatterer number. For four or more scatterers, the phase derivative PDF is well approximated by the prediction for a complex Gaussian process (22). The densities' heavy tails are due to the phase derivative 'spikes' that occur when the field encircles the origin, which is a well-known phenomenon in frequency demodulation [3]. J statistic densities for one and two scatterers are plotted in figure 7. The result for one scatterer is the same as the particle's phase shift derivative density (25), and the two-scatterer density matches the analytical prediction (33). For increasing scatterer number, the density broadens into a symmetric negative exponential, which agrees with the theoretical prediction (23) when $N = 6$, as seen in figure 9.

It is interesting that phase derivative spikes do not arise from two equal scatterers, when constructive interference can only produce field zeros, and not fields that pass through and encircle the origin. In fact, the case of exactly equal scatterers is a special one. In practice, any difference in the scattering amplitudes, or the presence of additive noise, will cause the resultant field to encircle the origin. This means that, in practice, the phase derivative variance will not be simply equal to one half of the variance of phase derivatives of the individual scatterers. For scattering amplitudes of unity and r, the phase derivative is given by

$$\dot{\phi} = \frac{J}{I} = \frac{\dot{\theta}_1 + r^2\dot{\theta}_2 + r(\dot{\theta}_1 + \dot{\theta}_2)\cos[\varphi]}{1 + r^2 + 2r\cos[\varphi]}. \tag{45}$$

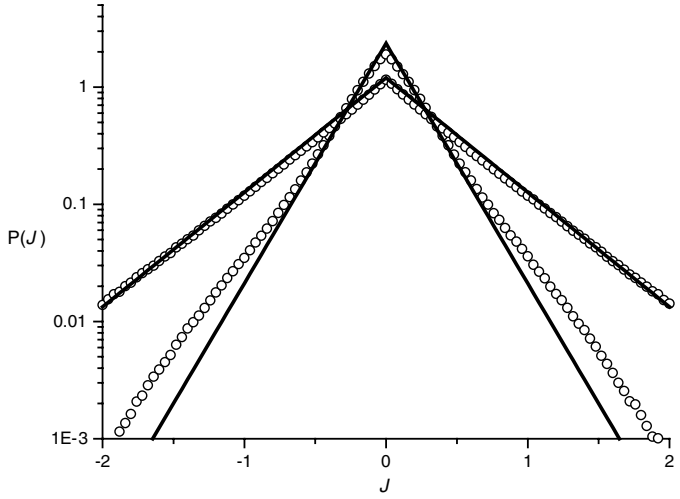

Figure 9. Same as figure 8 but for J statistic. The curves are theoretical predictions from equation (23) with $N = 3$ and 6, respectively. Note that the theoretical prediction scales with mean intensity $\langle I \rangle = N$.

The characteristic function of this variable can be averaged over the Gaussian distributed $\dot{\theta}_1$ and $\dot{\theta}_2$ and inverse Fourier transformed to yield the phase derivative density

$$p_2(\dot{\phi}|r) = \frac{1}{\pi\sqrt{2\pi\langle\dot{\theta}^2\rangle}} \int_0^\pi \mathrm{d}\varphi \frac{(1 + r^2 + 2r\cos[\varphi])}{\sqrt{(1 + r\cos[\varphi])^2 + (r^2 + r\cos[\varphi])^2}} \times \exp\left[-\frac{\dot{\phi}^2}{2\langle\dot{\theta}^2\rangle} \frac{(1 + r^2 + 2r\cos[\varphi])^2}{\{(1 + r\cos[\varphi])^2 + (r^2 + r\cos[\varphi])^2\}}\right]. \tag{46}$$

While analytical progress is difficult, the integral can be evaluated numerically for arbitrary r and can be shown to reduce to the expected limits when $r = 1$, i.e. two equal scatterers, and $r \to \infty$, i.e. effectively a single scatterer. The density (46) is plotted in figure 10 for various r. When $r > 1$, the density has a Gaussian body and heavier tails due to the origin encirclement phenomenon. The characteristic function of the J statistic follows from the numerator of (45) as

$$C_2(\lambda) = \langle \exp[\mathrm{i}\lambda(\dot{\theta}_1 + r^2\dot{\theta}_2)] J_0[\lambda r(\dot{\theta}_1 + \dot{\theta}_2)] \rangle, \tag{47}$$

where we have averaged over the uniformly distributed φ. Substituting the expression [21]

$$J_0(z) = \frac{1}{\pi} \int_0^\pi \exp[\mathrm{i}z\cos[\varphi]]\,\mathrm{d}\varphi \tag{48}$$

into (47) allows the averages over $\dot{\theta}_1$ and $\dot{\theta}_2$ to be performed. Application of an inverse Fourier transform returns the J statistic density

$$p_2(J|r) = \frac{1}{\pi\sqrt{2\pi\langle\dot{\theta}^2\rangle}} \int_0^\pi \mathrm{d}\varphi \frac{1}{\sqrt{(1 + r\cos[\varphi])^2 + (r^2 + r\cos[\varphi])^2}} \times \exp\left[-\frac{J^2}{2\langle\dot{\theta}^2\rangle\{(1 + r\cos[\varphi])^2 + (r^2 + r\cos[\varphi])^2\}}\right], \tag{49}$$

which also reduces to the expected limiting densities when $r = 1$ and $r \to \infty$. The integral can be evaluated numerically and is plotted in figure 11 for those same values of r evaluated

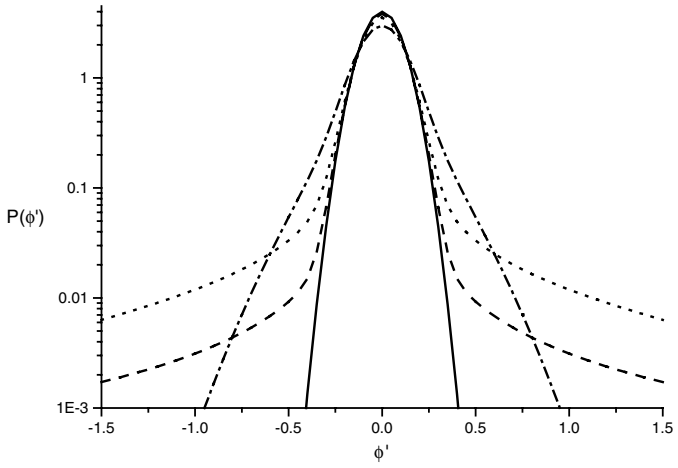

Figure 10. Phase derivative density from two scatterers with scattering amplitudes unity and $r = 1$ (solid line), $r = 1.01$ (dashed line), $r = 1.1$ (dotted line) and $r = 2$ (dash-dotted line).

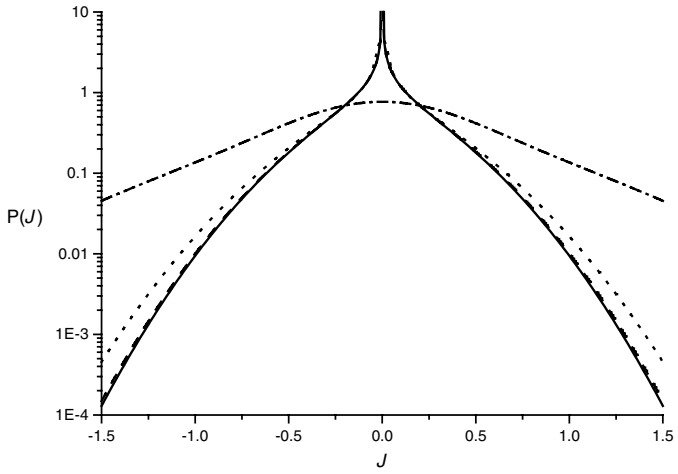

Figure 11. Same as figure 10 but for J statistic.

above. It is apparent that the J statistic density (49) is less sensitive than the phase derivative density (46) to small changes in the cross-sectional ratio r. This behaviour can also be inferred from (45), since as $r \to 1$ the phase derivative $\dot{\phi}$ can take on arbitrarily large values. However, in the limit when $r = 1$, the phase derivative $\dot{\phi}$ reduces to the prediction of equation (29). For three or more scatterers, small variations in the scattering amplitudes away from unity will be less significant because the resultant phasor is always able to encircle the origin.

Numerical simulation can also be used to investigate of the optimal form of amplitude weighting $f(A)$ when the field constitutes a non-Gaussian process. It was shown in [7] that for an arbitrary complex noise process, the optimal function of amplitude weighting is the reciprocal of the phase derivative's conditional variance, i.e.

$$f(A) = \langle \dot{\phi}^2 \rangle_A^{-1} = \left(\int_{-\infty}^{\infty} \dot{\phi}^2 \, p(\dot{\phi}|A) \, \mathrm{d}\dot{\phi} \right)^{-1}. \tag{50}$$

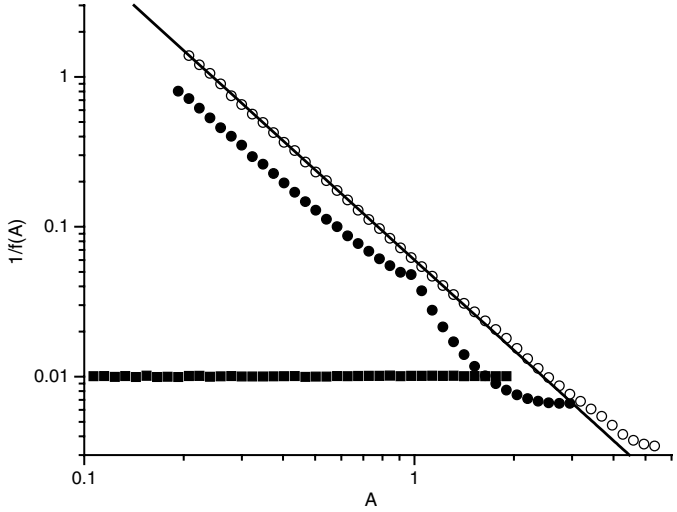

Figure 12. Optimal form of amplitude weighting $f(A)$ for two scatterers (squares), three scatterers (closed circles) and six scatterers (open circles). The solid line is the curve A^{-2} corresponding to intensity weighting.

When A and $\dot{\phi}$ are the amplitude and phase derivative of a complex Gaussian process [6], result (50) returns $\langle\dot{\phi}^2\rangle = 1/A^2$, confirming that the J statistic is ideal in this important case. To obtain $f(A)$ from simulation data, one stores amplitude values $A_{N,m} = \sqrt{I_{N,m}}$ in tandem with their corresponding phase derivative values $\dot{\phi}_{N,m}$. By using a suitable sorting algorithm, the amplitude values $A_{N,m}$ are arranged in order of magnitude, making sure that each value retains its associated phase derivative value $\dot{\phi}_{N,m}$. The sorted amplitude sequence is then split into segments, for which the corresponding phase derivative variance is evaluated. By minimizing the bin width of each amplitude segment, i.e. having a large number of bins over any given amplitude range, one obtains the variance of $\dot{\phi}$ conditional upon amplitude, i.e. $\langle\dot{\phi}^2\rangle_A$. This quantity is evaluated for two, three and six scatterers in figure 12. The curve for two scatterers indicates that the optimal amplitude weighting is A^0, i.e. no power of amplitude. This is because the phase derivative from two equal scatterers is independent of the field amplitude, which can be seen in equation (29). However, as mentioned above, two equal scatterers are somewhat idealistic, and in practice phase derivative spikes could arise from additional noise and slight differences in scattering amplitudes. When such spikes occur, some form of amplitude weighting will be appropriate to suppress their effects. The optimal weighting curve for three scatterers displays a discontinuity in the slope at unit amplitude, which is where the peak in figure 5(*b*) occurs, and exhibits an A^{-2} dependence at lower amplitude values. When more than three scatterers are present, the functional form of optimal weighting approximates intensity over the entire amplitude range, which is that result predicted for a complex Gaussian process.

6. Discussion and conclusions

In this paper, we investigated the phase derivative $\dot{\phi}$ and intensity-weighted phase derivative J returned from a two-dimensional random walk. The correlation properties and variance of J were obtained for the case of an unbiased random walk. Unlike in the case of a field scattered beyond a smoothly varying random phase screen [7], the normalized variance of

the J statistic was found to decrease monotonically and saturate to that result predicted for a complex Gaussian process. This suggests that intensity weighting can be adopted without incurring serious error under all fluctuation conditions generated by the random walk model. Furthermore, one might expect this assertion to apply more generally in diffusely scattered waves that do not exhibit heightened non-Gaussian intensity fluctuations. We also note that the correlation properties of the J statistic are proportional to the scatterers' phase shift derivative correlation function, i.e. $\langle\dot{\theta}(t)\dot{\theta}(t')\rangle$, and hence velocity correlation, which provides a means to determine certain properties of individual scatterers from the detected field.

By assuming that the positions, and resulting phase shifts, of individual scatterers are Gaussian distributed, probability densities were obtained for $\dot{\phi}$ and J from one and two scatterers. These results were found to be in excellent agreement with numerical simulation, which was then used to investigate the field returned from a larger number of scatterers. The phase derivative density for three scatterers was found to possess heavy tails, and the density for a larger number of scatterers converges rapidly to that result predicted for a complex Gaussian process. The J statistic densities were also found to converge rapidly to the Gaussian prediction. The optimal function of amplitude weighting was determined from simulation data, and the results confirm that intensity weighting can be adopted for arbitrary scatterer number without incurring serious error.

While the amplitude and intensity properties of two-dimensional random walks have received considerable attention in the context of scattered coherent radiation, few results exist for their phase-related properties beyond the Gaussian limit. The results of this paper should therefore find utility in phase sensitive detection and frequency retrieval from radiation scattered by random media. It is worthwhile noting that a closely related problem arises in the spatial domain in radars, where angular 'glint' errors reduce the radars ability to track the target barycentre [25, 26].

References

[1] Middleton D 1996 *An Introduction to Statistical Communication Theory* (New York: IEEE)
[2] Wheelon A D 2005 *Electromagnetic Scintillation: I. Geometrical Optics* (Cambridge: Cambridge University Press)
[3] Taub H and Schilling D 1971 *Principles of Communication Systems* (New York: McGraw-Hill)
[4] Miller J F, Schatzel K and Vincent B 1991 The determination of very small electrophoretic mobilities in polar and non-polar colloidal dispersions using phase analysis light scattering *J. Colloid Interface Sci.* **143** 532–54
[5] Ridley K D and Jakeman E 1999 FM demodulation in the presence of multiplicative and additive noise *Inverse Problems* **15** 989–1002
[6] Rice S O 1948 Statistical properties of a sine wave plus random noise *Bell Syst. Tech. J.* **27** 109–57
[7] Jakeman E, Ridley K D and Watson S M 2001 Intensity-weighted phase derivative statistics *J. Opt. Soc. Am.* A **9** 2121–31
[8] Wax N 1954 *Selected Papers on Noise and Stochastic Processes* (New York: Dover)
[9] Jakeman E and Tough R J A 1998 Non-Gaussian noise models for the statistics of scattered waves *Adv. Phys.* **37** 471–529
[10] Booker H G, Ratcliffe J A and Shinn D H 1950 Diffraction from an irregular screen with applications to ionospheric problems *Phil. Trans. R. Soc.* A **242** 579–607
[11] Uscinski B J (ed) 1986 *Wave Propagation and Scattering* (Oxford: Clarendon)
[12] Beckman P and Spizzichino A 1963 *The Scattering of Electromagnetic Waves from Rough Surfaces* (Oxford: Pergamon)
[13] Pearson K 1905 The problem of the random walk *Nature* **72** 294–5
[14] Cummins H Z and Pike E R (ed) 1973 *Photon Correlation and Light Beating Spectroscopy* (New York: Plenum)
[15] Ishimaru A 1978 *Wave Propagation and Scattering in Random Media* (New York: Academic)
[16] Morse P M and Feshbach H 1953 *Methods of Theoretical Physics* (New York: McGraw-Hill)
[17] Kachelmyer A L and Schultz K I 1995 Laser vibration sensing *Linc. Lab. J.* **8** 3–28

[18] Bastiaans M and Wolf K 2003 Phase reconstruction from intensity measurements in linear systems *J. Opt. Soc. Am.* A **20** 1046–9
[19] Siegert A J F 1943 *MIT Rad. Lab. Rep. No* 463
[20] Barakat R 1986 Weak scatter generalisation of the K-density function with application to laser scattering in atmospheric turbulence *J. Opt. Soc. Am.* A **3** 401–9
[21] Abramowitz M and Stegun I A 1972 *Handbook of Mathematical Functions* (New York: Dover)
[22] Kluyver J C 1905 A local probability problem *Proc. K. Ned. Akad. Wet.* **14** 341–50
[23] Goodman J W 1985 *Statistical Optics* (New York: Wiley–Interscience)
[24] Watts T R, Hopcraft K I and Faulkner T R 1996 Single measurements on probability density functions and their use in non-Gaussian light scattering *J. Phys. A: Math. Gen.* **29** 7501–17
[25] Delano R H 1953 A theory of target glint or angular scintillation in radar tracking *Proc. IRE* **41** 1778–84
[26] Le Chevalier F 2002 *Principles of Radar and Sonar Signal Processing* (Boston, MA: Artech House Publishers)